Illuminating the Human Metabolome: Selective Detection of Multiple Metabolites in Unaltered Biofluids via Hyperpolarisation-Enhanced NMR Spectroscopy

Lars T. Kuhn,[1,*] Stefan Weber,[1] Joachim Bargon,[2] Teodor Parella,[3] and Míriam Pérez-Trujillo[3,*]

[1]Institut für Physikalische Chemie, Albert-Ludwigs-Universität Freiburg, Albertstr. 21, 79104 Freiburg i. Br. (Germany); [2]Institut für Physikalische und Theoretische Chemie, Rheinische Friedrich-Wilhelms-Universität Bonn, Wegelerstr. 12, 53115 Bonn (Germany); [3]Servei de Ressonància Magnètica Nuclear, Facultat de Ciències i Biociències, Universitat Autònoma de Barcelona, 08193 Cerdanyola del Vallès, Catalonia (Spain)

Abstract: Detecting and identifying individual metabolites in biological mixtures constitutes a challenge in analytical research. In this context, nuclear magnetic resonance (NMR) has proven to be powerful providing precise qualitative and quantitative information non-invasively. However, NMR is inherently insensitive and lacks selectivity regarding the analysis of molecular targets in complex mixtures. Here, we present a method that circumvents these shortcomings performing photo-chemically induced dynamic nuclear polarisation (photo-CIDNP) on unmodified biofluids, i.e. human urine and serum. We demonstrate that photo-CIDNP on biofluids is feasible, can be performed straightforwardly in the native aqueous medium at physiological concentrations, and acts as a spectral filter highlighting a clinically relevant metabolite subset. The method is compatible with standard metabolomics protocols and holds great promise for in-depth studies for use in metabolomics and other areas of analytical research.

Introduction

The simultaneous detection and identification of a multitude of chemically and structurally very different analytes present in complex biological mixtures has gained significant relevance in recent years. In particular, the advent of the rapidly growing field of metabolomics research [1,2] has highlighted the need for automated high-throughput analytical methods that allow the concurrent analysis of multiple metabolites in complex biofluids. In this context, nuclear magnetic resonance (NMR) spectroscopy has emerged as a key analytical technique given its ability to extract extremely precise qualitative and, in many cases, also quantitative information on numerous metabolites simultaneously in a fully non-invasive manner. Thus, the method has found wide applicability in areas such as metabolism studies and metabolic profiling as well as many other disciplines where complex biological mixtures containing, for example, clinically relevant metabolites require efficient characterisation [3].

Despite of the advantages NMR offers compared to other analytical platforms, e.g. mass spectrometry, its inherent sensitivity is low. Hence, a variety of different methodological improvements has been developed over the last decades to overcome this drawback. These range from the introduction of higher magnetic fields and cryogenically cooled NMR probes to other, more exotic, setup modifications such as the use of microfluidics and NMR microcoil detection methods as well as combinations thereof [4]. Another strategy that has been pursued to substantially increase the detection limit of NMR is the application of so-called hyperpolarisation methods, i.e. physical or

[*]To whom correspondence should be addressed: Lars T. Kuhn (lars.kuhn@physchem.uni-freiburg.de), Institut für Physikalische Chemie, Albert-Ludwigs-Universität Freiburg, Albertstr. 21, 79104 Freiburg i. Br. (Germany) & Míriam Pérez-Trujillo (miriam.perez@uab.cat), Servei de Ressonància Magnètica Nuclear, Facultat de Ciències i Biociències, Universitat Autònoma de Barcelona, 08193 Cerdanyola del Vallès, Catalonia (Spain)

chemical means to increase the signal-to-noise ratio of an NMR measurement performed in liquids. Amongst those, dissolution dynamic nuclear polarisation (d-DNP) [5] as well as hydrogenative and non-hydrogenative parahydrogen-induced polarisation procedures (PHIP and NH-PHIP) [6] have featured most prominently in recent years.

Both d-DNP and PHIP have also been employed to facilitate the study of complex biological mixtures. For example, Tessari and co-workers utilised non-hydrogenative PHIP in order to detect and quantify α-amino acids in human urine following dilution of the sample with methanol in the presence of an iridium-based pre-catalyst [7]. In another study, Dey *et al.* presented an untargeted NMR-based metabolomic workflow based on dissolution DNP thereby enabling hyperpolarised ^{13}C metabolomics of plant extracts at natural abundance [8]. Despite of these and several other [9,10] extremely encouraging results, typical liquid-state NMR experiments employing d-DNP- or parahydrogen-based hyperpolarisation will, most likely, have a limited applicability in metabolomics research due the very specific and demanding sample preparation/setup requirements, e.g., harsh hyperpolarisation conditions and/or long polarisation times in combination with the occasional need for expensive additional instrumentation, which render biocompatible and automated high-throughput NMR measurements rather difficult.

Photochemically-induced dynamic nuclear polarisation (photo-CIDNP), another nuclear spin-selective technique, uses somewhat milder, i.e. less invasive, experimental conditions and involves the instantaneous (low-power) LED- or laser light-induced generation of transient radical pairs in the presence of a small amount of a photosensitiser yielding spin-polarised molecular species [11-13]. In addition, photo-CIDNP is a very sensitive homo- and heteronuclear hyperpolarisation method that allows the NMR detection of analytes present in a low nanomolar concentration range provided that certain experimental requirements are met [14,15]. Traditionally, the method has been mainly employed to gauge bio-macromolecular solvent exposure in the steady state as well as in real-time owing to its ability to selectively highlight the three aromatic amino acid side-chains of tyrosine (Tyr), tryptophan (Trp), and histidine (His) as well as the aliphatic amino acid methionine (Met). Thus, up to the present, biological photo-CIDNP experiments have been conducted almost exclusively for the analysis of isolated amino acids and proteins in buffered aqueous solution. To the best of our knowledge, only one precedent of the application of photo-CIDNP NMR spectroscopy in the context of (complex) biological media has been reported using specific means, which seem difficult to be implementable into metabolomic workflows: the detection of a singly ^{13}C-labelled Trp isotopologue in a diluted bacterial cell extract applying a low concentration (LC) photo-CIDNP approach involving multi-step pretreatment procedures of the sample solution prior to acquisition of the hyperpolarisation spectrum [14,15].

Here, we demonstrate the feasibility of conducting liquid-state photo-CIDNP NMR experiments for the direct and very selective analysis of complex biological mixtures, i.e. human urine and serum, in a rapid, minimally invasive manner thereby avoiding any chemical or physical modification of the original biofluid prior to the analysis. To achieve this, we employed a specific one-dimensional photo-CIDNP NMR pulse sequence that yields background-free hyperpolarisation NMR spectra featuring signal-enhanced metabolite resonances exclusively within a few

seconds of measurement time. Furthermore, the substantial analytical potential of the method is highlighted given that – out of a reservoir of a myriad of different small-molecule components – only a specific subset of clinically relevant targets, i.e., Trp, Tyr, His, Met, and, most interestingly, several additional metabolites, can be detected straightforwardly in their native environment. In addition, we explain how the method can be easily extended to allow for the high-throughput analysis of a large, metabolomically relevant number of samples, thereby underscoring the significant analytical capabilities of the approach.

Results and Discussion

In order to test the feasibility of performing photo-CIDNP experiments on unmodified complex fluids of biological origin, we decided to pursue a sequential experimental strategy: (i) prior to performing photo-CIDNP NMR studies of untreated human urine and serum samples, the feasibility of recording photo-CIDNP NMR spectra of multiple molecules present in a molecularly congested environment using our setup was explored. To achieve this, we carried out the experiment using an aqueous complex mixture of the twenty naturally occurring L-amino acids; (ii) in a second step, the same experiment was conducted on a sample of normal human urine enriched with the four photo-CIDNP-active amino acids Tyr, Trp, His, and Met; (iii) third, the acquisition of a 1D photo-CIDNP NMR spectrum of a completely untreated sample of normal human urine was performed; (iv) finally, steps (ii) and (iii) were repeated examining amino acid-doped and pristine samples of human serum, respectively.

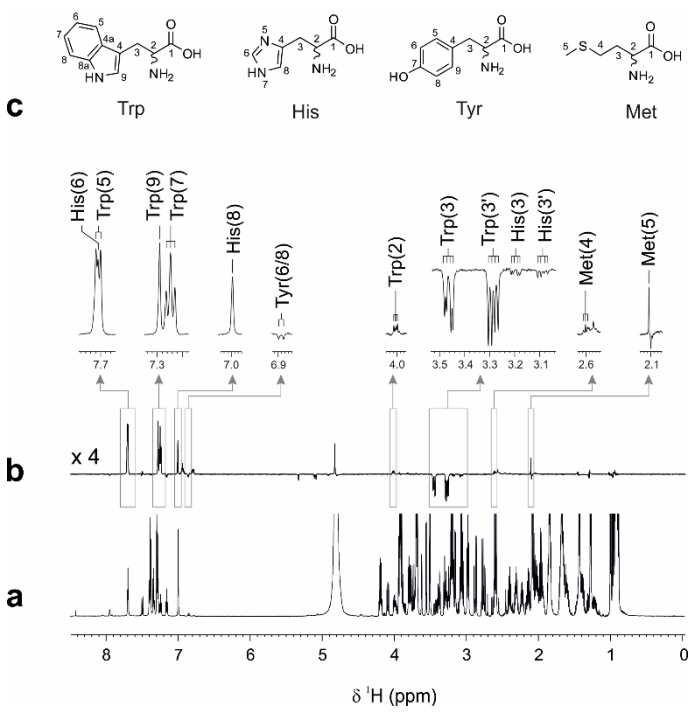

Figure 1. Comparison of one-dimensional (a) ^{1}H and (b) ^{1}H photo-CIDNP NMR spectra of "mixture 1" (pH 7.2). In the upper part, expanded aliphatic and aromatic regions of the ^{1}H photo-CIDNP spectrum are shown together with the respective resonance assignments. (c) Molecular structures of tryptophan, histidine, tyrosine, and methionine together with the respective numbering scheme used for all ^{1}H nuclei. All experiments were conducted with 16 scans and a recycle delay (d1) of 3 s (c.f. Supporting Information).

In a first step, an aqueous mixture (mixture 1) was prepared containing the twenty naturally occurring amino acids in a low, physiologically representative concentration (c.f Supporting Information, Table S1). To this, a small

amount of the photosensitiser flavin mononucleotide (FMN; c = 0.2 mM) – essential for observing the biomolecular photo-CIDNP effect – was added, and then both thermal and photo-CIDNP ^{1}H NMR experiments were conducted. For the acquisition of all hyperpolarisation spectra described here, a specific one-dimensional ^{1}H photo-CIDNP NMR pulse sequence developed by Hore and co-workers was used, which yields a "pure" photo-CIDNP spectrum and, thus, renders the subsequent subtraction of photo-CIDNP "light" and "dark" spectra superfluous [16]. The experiment combines presaturation of (thermal) background magnetisation by a string of composite π/2 pulses, each followed by a defocusing field gradient, and subsequent gated illumination during a grid of π pulses with a prescribed timing. This permits the acquisition of clean photo-CIDNP spectra that are free from background magnetisation thereby avoiding the sensitivity loss and subtraction artefacts associated with difference spectroscopy. The latter is of particular importance when analysing 1D photo-CIDNP data of complex mixtures given that the presence of a large number of different metabolite resonances in both photo-CIDNP "light" and "dark" spectra can lead to multiple spectral subtraction imperfections that significantly hinder the accurate analysis of such data. Each photo-CIDNP NMR spectrum shown here was acquired with 16 scans and a laser illumination time of 350 ms per scan using a state-of-the-art continuous wave diode laser (max. nominal output power: 400 mW) emitting at a wavelength (λ) of 445 nm (c.f. Supporting Information). Figure 1 compares the thermal ^{1}H NMR spectrum of mixture 1 (Figure 1a) with the photo-CIDNP NMR spectrum of the same sample (Figure 1b), exclusively highlighting hyperpolarised amino acid nuclei resonances.

While the thermal ^{1}H NMR spectrum of mixture 1 (Figure 1a) shows a multitude of partially overlapping NMR signals, the acquisition of the photo-CIDNP NMR data of the same sample yields a clean, background-free spectral output showing only the hyperpolarised signals of the four photo-CIDNP-active amino acids (Figure 1b). In particular, protons H2, H5, H7 and H9 of tryptophan show absorptive polarisation whereas the two β-CH_2 nuclei, H3 and H3', are emissively polarised. In the case of histidine, the aromatic ring protons H6 and H8 exhibit absorptive polarisation while the polarisation signals representing the β-CH_2 protons are weakly emissive. Furthermore, absorptive polarisation for the H4 and H5 protons of the aliphatic amino acid methionine is observed. In the case of tyrosine – present in a much lower concentration in mixture 1 than the other three photo-CIDNP-active amino acids – only the emissively polarised H6,8 protons can be detected. This observation is consistent with the polarisation pattern found in ^{1}H photo-CIDNP NMR spectra of isolated tyrosine, typically characterised by a strong emissive polarisation for the aromatic ring protons H6,8 and only relatively weak absorptive polarisation signals for the aromatic H5,9 and the β-CH_2 nuclei.

Hence, we were able to hyperpolarise simultaneously Tyr, Trp, His, and Met within a relatively complex aqueous mixture containing numerous other, non-polarisable metabolites employing our photo-CIDNP NMR setup. Moreover, the polarisation pattern of the individual amino acid resonances as well as their sign, i.e. emissive or absorptive, and the relative signal intensities resemble those found in photo-CIDNP NMR spectra of the isolated aromatic amino acids recorded in the absence of cosolutes [12,17]. Interestingly, all four photo-CIDNP active amino acids were hyperpolarised simultaneously although other, structurally similar molecules were present in the mixture. In principle, these could also have interacted with the FMN photosensitiser thereby preventing or

attenuating the generation of photo-CIDNP. As such, this preliminary result gave reason to believe that hyperpolarisation of the four photo-CIDNP-active amino acids might also be observable in more complex, metabolomically relevant, environments.

In a subsequent step, both thermal and ^{1}H photo-CIDNP NMR spectra of a sample of normal human urine (pH 6.8) – taken from a healthy volunteer – spiked with the four photo-CIDNP-active amino acids ("spiked urine 1": *c* (Trp): 0.043 mM; *c* (His): 0.341 mM; *c* (Tyr): 0.011 mM; *c* (Met): 0.350 mM; *c* (FMN): 0.2 mM) were recorded (Figure 2). As expected, the thermal ^{1}H NMR spectrum of this mixture (Figure 2a) is characterised by the presence of a large number of NMR signals of very different intensities thereby reflecting the wide range of metabolite concentrations found in normal human urine. Furthermore, many of these signals show considerable overlap which renders the detection and identification of poorly concentrated metabolites difficult. In contrast, the photo-CIDNP spectrum of the same sample (Figure 2b) shows numerous hyperpolarised NMR resonances, while all other NMR signals present in the thermal spectrum are absent. A straightforward analysis allowed the identification of most of these hyperpolarised NMR resonances by comparison of the respective chemical shifts with reported literature values and/or their characteristic polarisation signal pattern. In particular, polarised signals were attributed to ^{1}H nuclei of either histidine (polarised ^{1}H nuclei: H6, H8), tryptophan (H2, H3, H3', H5, H7, and H9), tyrosine (H6,8), or methionine (H4, H5). While hyperpolarisation signals representing the aliphatic beta-protons of tyrosine and histidine are absent in this spectrum, several additional polarisation signals of unknown origin – marked with an asterisk in Figure 2b – can clearly be identified.

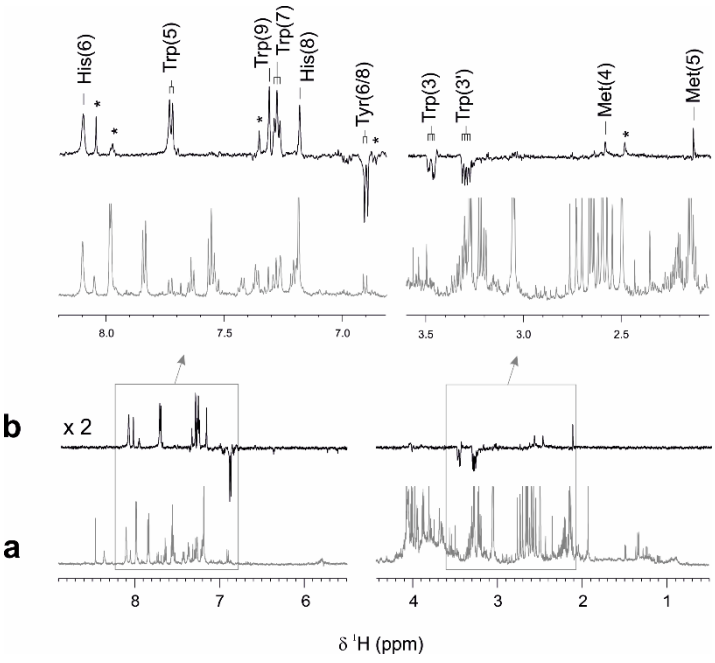

Figure 2. Comparison of one-dimensional (a) ^{1}H and (b) ^{1}H photo-CIDNP NMR spectra of "spiked urine 1" (pH 6.8). In the upper part, expanded aliphatic and aromatic regions of both spectra are shown together with the respective resonance assignments. Unassigned hyperpolarised resonances are marked with an asterisk (see text). All experiments were conducted with 16 scans and a recycle delay (d1) of 3 s (c.f. Supporting Information).

Thus, the analysis of these data clearly shows that hyperpolarisation of the four polarisable amino acids via the photo-CIDNP effect can be detected in a complex biofluid, e.g. human urine, and that its complex biological matrix does not hinder the hyperpolarisation of these metabolites. This finding is anything but trivial given that, for

example, the specific and non-specific binding of the lowly concentrated photosensitiser (FMN; c = 0.2 mM) or the four polarisable amino acids to other, photo-CIDNP-inactive molecular, ionic and/or complexing components as well as the competition for excited triplet FMN species between the four photo-CIDNP-active amino acids and other molecular species found in human urine – to date, several thousand different components have been identified in human urine [18] – could, in principle, have prevented the detection of polarisation signals entirely [17,19].

Encouraged by these results, we then recorded both thermal and photo-CIDNP ^{1}H NMR spectra of a completely untreated sample of human urine ("urine 2") in the presence of the photosensitiser FMN (c = 0.2 mM) (Figure 3). A first analysis of the data shows that the photo-CIDNP ^{1}H NMR spectrum of the pristine urine sample (Figure 3b) yields a much cleaner, i.e. background-free, result as compared to its thermal counterpart (Figure 3a). Moreover, it is significantly different from the hyperpolarised NMR spectra obtained for both "mixture 1" and "spiked urine 1" (Figure 1b and Figure 2b). Whereas the aliphatic part of the photo-CIDNP spectrum shown in Figure 3b hardly exhibits any signals, its aromatic region features a relevant number of hyperpolarised NMR resonances (U1 to U5) that have not been detected before and whose chemical shift positions differ from those assigned in Figure 1b and Figure 2b, respectively (see below). In addition, hyperpolarised resonances of the aromatic amino acids tyrosine (H6,8) and tryptophan (H5, H7, H9) are also detectable (c.f. Fig. 3b). In contrast, signals of histidine and methionine are completely absent in the spectrum. This finding can most likely be attributed to a lower concentration of these species in the sample. Also, the absence of these signals might be due to the fact that, unlike Tyr and Trp, both His and Met compete less favourably for the amount of triplet-excited flavin molecules present in solution after each laser flash [17]. This, in turn, would lead to a less pronounced photo-CIDNP effect in the resulting spectrum.

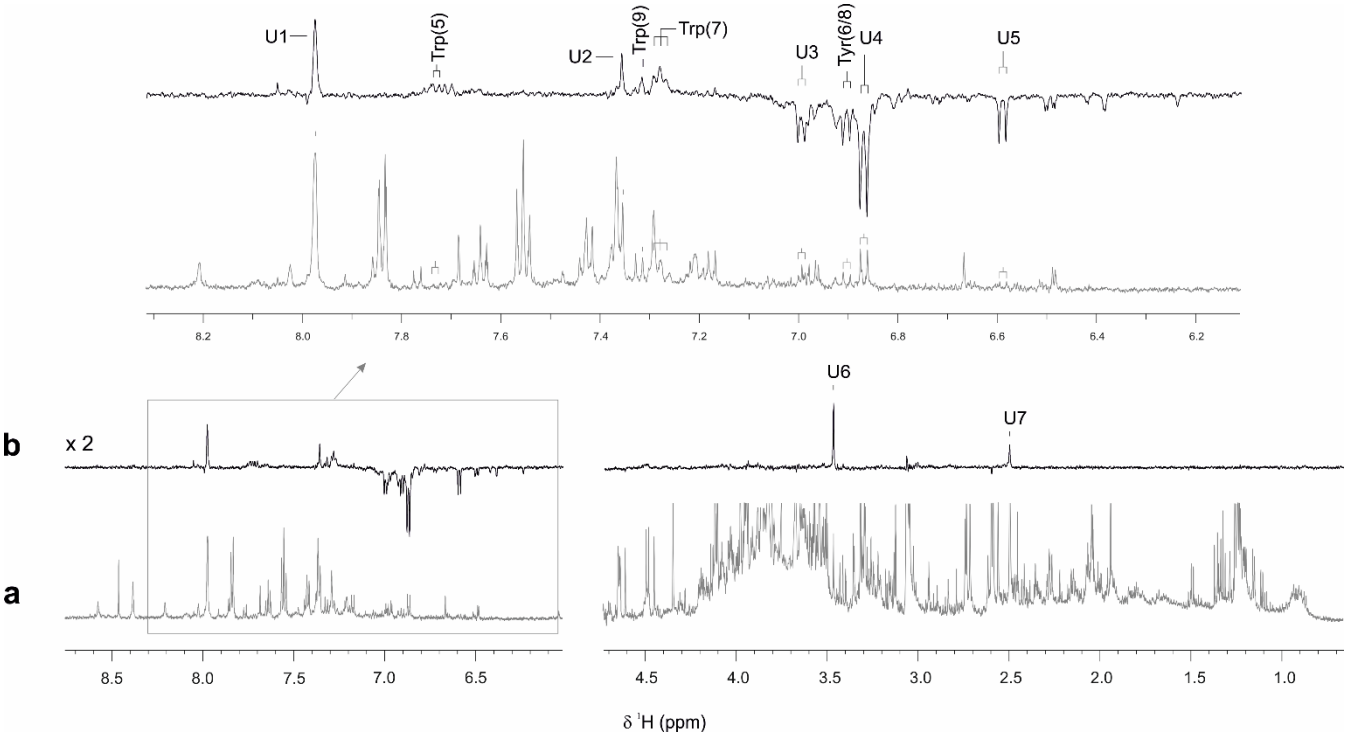

Figure 3. Comparison of one-dimensional (a) ^{1}H and (b) ^{1}H photo-CIDNP NMR spectra of an untreated sample of normal human urine, "urine 2" (pH 6.8). In the upper part, an expanded section of the aromatic region of both spectra is highlighted. Assignments for hyperpolarised Tyr and Trp resonances are indicated and a numbering scheme for the most intense unidentified hyperpolarised signals (U1-U7) is shown (see text). All experiments were conducted with 16 scans and a recycle delay (d1) of 3 s (c.f. Supporting Information).

A more detailed analysis of the aromatic region of the hyperpolarisation spectrum shown in Figure 3b identifies a number of emissive doublet signals (U3 to U5) located both 'upfield' and 'downfield' from the emissive resonance representing the H6,8 protons of tyrosine. Interestingly, most of these resonances are hardly observable in the thermal ^{1}H NMR spectrum of the sample. Even though a complete structural analysis of these species lies beyond the scope of the exploratory study presented here, an educated guess can be made regarding the structural and/or metabolic origin of these signals. Given that tyrosine is the only known photo-CIDNP-active amino acid that exhibits negative enhancements in the aromatic region of the NMR spectrum, these additional emissive resonances can possibly be attributed to tyrosine derivatives – or, alternatively, other metabolites containing a *para*-substituted aromatic ring structure – that form part of tyrosine/phenylalanine metabolism. For example, the chemical shift value of signal U4 in combination with its aromatic TOCSY pattern (see Supporting Information; Figure S1) is consistent with the chemical structures of 4-hydroxyphenylpyruvic acid, 4-hydroxyphenyllactic acid, and 4-hydroxyphenylacetic acid, respectively [20]. Interestingly, these three metabolites function as biological molecular markers for certain medical conditions. For example, their upregulation in neonatal urine seems to indicate type II/III tyrosinemia [21]. As far as the analysis of other hyperpolarised resonances found in the photo-CIDNP spectrum is concerned, resonance assignment can be made with respect to the two hyperpolarised singlets found at δ = 7.98 ppm (U1) and δ = 7.36 ppm (U2), respectively, which, besides, were also observed in the photo-CIDNP spectrum of "spiked urine 1". Their chemical shift position points to the histidine metabolites 1- and/or 3-methylhistidine – known to exhibit photo-CIDNP enhancements [22] – which are important intermediates in histidine metabolism. Furthermore, aberrant levels of these metabolites found in different human body fluids are indicative of a number of medical conditions, e.g. kidney disease, early and late-onset preeclampsia, Alzheimer's disease, and type 2 diabetes mellitus [20,23]. Additional hyperpolarised NMR signals, i.e., U6 and U7, as well as several other, less intense resonances not highlighted in Figure 3 were also detected in the photo-CIDNP spectrum of "urine 2". Further evaluation of these and other potentially polarised metabolites found in this sample of normal human urine lies beyond the scope of this exploratory work and will be part of future investigations.

In a final step, we investigated if the photo-CIDNP technique can also be applied to analytes present in metabolomically relevant matrices other than urine. Thus, the observation of photo-CIDNP in both amino acid-doped and fully untreated samples of normal human serum [24] following identical procedures as described before was explored (c.f. Supporting Information). With regard to performing NMR experiments requiring sample illumination, we encountered that undiluted human serum is a rather challenging medium given that it is often, unlike urine, not fully transparent but rather turbid – serum turbidity is usually caused by the cryoprecipitation of lipid components during freezing and thawing cycles – resulting in a relatively high optical density of the sample solution. Accordingly, the laser light exiting the tip of the optical fibre does not penetrate the entire active volume of the NMR sample thereby producing less triplet-excited photosensitiser molecules upon illumination. Thus, we expected that the photo-CIDNP effect should be less pronounced as compared to the abovementioned results achieved with human urine samples [25].

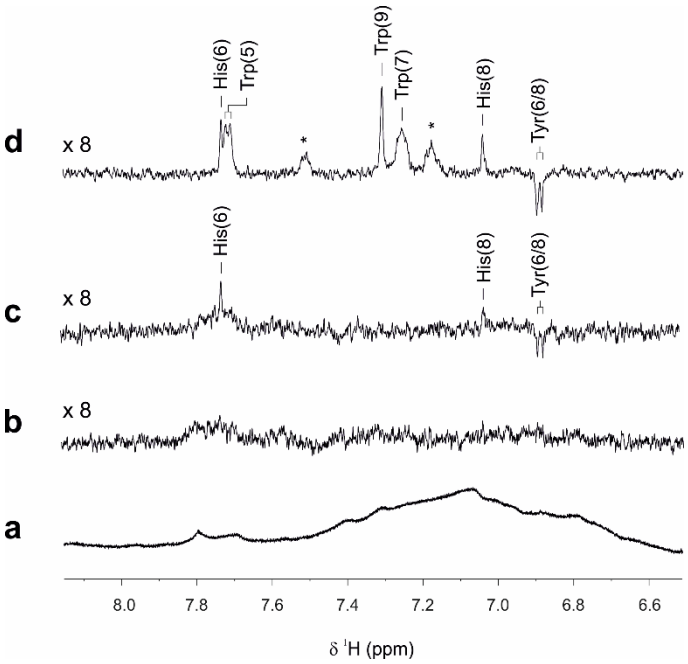

Figure 4. Comparison of the aromatic regions of (a) ^{1}H, (b) ^{1}H CPMG, and (c) ^{1}H photo-CIDNP NMR spectra of a pristine sample of normal human serum (pH 7.2). In addition, the aromatic region of (d) a ^{1}H photo-CIDNP NMR spectrum of an amino acid-doped serum sample is shown. Resonance assignments of hyperpolarised signals found in the photo-CIDNP spectra are indicated. Unidentified polarisation signals are marked with an asterisk (see text). All experiments were conducted with 16 scans and a recycle delay (d1) of 3 s (c.f. Supporting Information).

Figure 4 compares the aromatic regions of the photo-CIDNP spectra of unmodified (Figure 4c) human serum ("serum 1") and the amino acid-doped serum sample ("spiked serum 1": *c* (Trp): 0.520 mM; *c* (His): 0.341 mM; *c* (Tyr): 0.022 mM; *c* (Met): 0.350 mM; *c* (FMN): 0.2 mM; Figure 4d). In addition, 1D ^{1}H (Figure 4a) and ^{1}H Carr-Purcell-Meiboom-Gill (CPMG) (Figure 4b) NMR spectra of the unmodified serum sample acquired prior to conducting the photo-CIDNP experiment are shown for comparison [26]. While the aromatic region of the ^{1}H NMR spectrum of untreated human serum is characterised by broad signals originating from high-molecular-weight components, e.g. proteins and lipids, typically found in this medium, acquisition of a state-of-the-art ^{1}H CPMG experiment yields an aromatic spectral region void of any signals.

Interestingly, both photo-CIDNP spectra shown in Figure 4c and 4d, respectively, do clearly feature polarisation-enhanced NMR signals in the aromatic region – albeit smaller than those detected in samples of human urine – corresponding to photo-CIDNP-active amino acids. In particular, the polarisation spectrum representing the amino acid-doped sample exhibits significantly broadened photo-CIDNP signals for Tyr, His, and Trp. However, no signals can be observed for the amino acid methionine. This observation can possibly be attributed to a less favourable competition of Met for triplet-excited FMN molecules [17]. In addition, two unassigned hyperpolarised NMR signals – indicated with asterisks in Figure 4d – were also detected. Interestingly, their chemical shift positions coincide with those for Trp's H6 and H8 protons which can normally not be polarised via the photo-CIDNP effect (c.f. Supporting Information, Figure S2). With regard to the unaltered serum sample, weakly hyperpolarised His (H6 and H8) and Tyr (H6/8) resonances were detected. Importantly, these signals are entirely absent in the ^{1}H CPMG spectrum (Figure 4b) acquired prior to conducting the photo-CIDNP experiment. Furthermore, polarisation signals stemming from other metabolites, e.g. Trp and Met, cannot be observed in the

spectrum. This finding is most likely due to a substantially lower concentration of these species in this sample of human serum.

Conclusion

Here, we have demonstrated that the acquisition of 1D ^{1}H photo-CIDNP NMR data of unmodified samples of human urine and serum is feasible, can be accomplished in a minimally-invasive manner, i.e. hyperpolarisation is generated within the analyte molecules in their native biological matrix, and yields a clean, background-free spectral output featuring photo-CIDNP-enhanced NMR signals of the amino acids tyrosine, tryptophan, histidine and methionine. Interestingly, our study also showed that other metabolites found in human biofluids can be hyperpolarised as well using this method. The specific detection and identification of these species as part of a metabolomic analysis is of importance given their high clinical significance for the diagnosis and treatment of different pathologies, e.g. Alzheimer's Disease [27], Lewy body dementia [28], Parkinson's Disease [29], and leukemia [30]. Furthermore, the method is fast, robust, and yields highly reproducible results. Two additional characteristics of this analytical approach are of great importance in the context of metabolomic studies – and generally in the analysis of biological samples – as they facilitate the comparison and identification of metabolites with current spectral databases: (i) all hyperpolarised metabolite signals appear at identical chemical shift positions in the spectrum as compared to the original sample; (ii) although we did not add any type of standard buffer, e.g. phosphate, in this study, the photo-CIDNP method allows its use to control the pH of the medium [17]. We believe that no other NMR hyperpolarisation technique has, as of yet, achieved a similar level of compatibility with general analytical procedures for the study of biological samples, Accordingly, the work presented here opens a new branch of research in the field of hypersensitive NMR analyses of complex biological mixtures. In particular, it will enable the development of new applications in the field of metabolic profiling and metabolomic studies, as well as in other areas where complex mixtures containing clinically relevant metabolites need to be efficiently characterised. Due to its non-invasive character and the relatively modest setup requirements, a straightforward incorporation of the approach into existing NMR-based metabolomic workflows seems likely.

The photo-CIDNP method as applied to unmodified biofluids bears a significant analytical potential and, thus, numerous lines of investigation should be pursued in future studies to improve its overall performance. First, the detection limit of the technique needs to be lowered. Significant experimental and theoretical work into increasing the sensitivity of biological photo-CIDNP NMR measurements has been carried out by the group of Cavagnero in the last fifteen years. It has very recently been demonstrated that a combination of some of these setup improvements can lower the photo-CIDNP detection limit down to the low nM concentration range [14,15]. Many of these improvements can be implemented into the photo-CIDNP analysis of metabolomically relevant biofluids. Second, a class of polarisable molecular targets needs to be identified. In general, the photo-CIDNP effect is limited to molecules with low ionisation energies, e.g aromatics, able to participate in the Radical Pair Mechanism (RPM) responsible for the generation of CIDNP [17]. Hence, biological photo-CIDNP was known to be mainly restricted to the four amino acids tyrosine, tryptophan, histidine and methionine. This work has shown that at least several

additional metabolites can also be polarised via the photo-CIDNP effect. As such, it has to be explored whether other (aromatic) metabolites can be polarised as well. Given that a relevant number of newly identified photo-CIDNP-active small molecules has been reported very recently [31] we believe that the approach might be applied as a more general metabolomics screening method in the future. In particular, its use might be of significant benefit for targeted metabolomics analyses as the method's substrate selectivity can be further increased by variation of the photo-CIDNP photosensitiser and/or the pH of the sample solution [17]. Third, means to incorporate the method into metabolomic workflows need to be found and studies into the quantifiability of photo-CIDNP signals stemming from polarisable metabolite molecules present in complex biofluids have to be carried out. This would extend the method to allow for a reliable high-throughput screening of a metabolomically relevant number of samples. Finally, we believe that our approach can be merged with low-field detection methods (e.g. NMR benchtop solutions). The advantages of this will be two-fold: i) the photo-CIDNP effect is more pronounced at lower magnetic field strengths than used here. Hence, the polarisation of analytes at these lower field strengths should, in principle, yield higher amounts of nuclear polarisation; ii) the introduction of benchtop NMR solutions facilitates the use of (automated) flow-probe-assisted on-line reaction monitoring *in situ*. In addition, a fiberless "NMR torch" illumination protocol [32] would be combinable with such an approach.

Acknowledgements

We want to particularly acknowledge the donors and the Biobank Biobanco Hospital Universitario de La Princesa (ISCIII B.0000763) for their collaboration. Financial support provided by the Spanish Ministry of Economy and Competitiveness (project PGC2018-095808-B-I00) is also gratefully acknowledged. Furthermore, we thank the "Servei de Ressonància Magnètica Nuclear" (SeRMN) of the Universitat Autònoma de Barcelona (UAB) for the provision of spectrometer time.

Keywords

analytical methods, biofluids, hyperpolarisation, metabolite analysis, NMR spectroscopy

Conflict of Interest

All authors declare that they have no conflicts of interest.

References

1. D. S. Wishart (**2019**) *Phys. Rev.* 99:1819-1875
2. C. H. Johnson, J. Ivanisevic, G. Siuzdak (**2016**) *Nat. Rev. Mol. Cell. Biol.* 17:451-459
3. *NMR-based Metabolomics* (Ed.: H. C. Keun) The Royal Society of Chemistry, Cambridge, **2018**

4. J. Eills, W. Hale, M. Utz (**2022**) *Prog. Nucl. Magn. Reson. Spectrosc.* 128:44-69
5. S. J. Elliott, Q. Stern, M. Ceillier, T. El Daraï, S. F. Cousin, O. Cala, S. Jannin (**2021**) *Prog. Nucl. Magn. Reson. Spectrosc.* 126-127:59-100
6. R. A. Green, R. W. Adams, S. B. Duckett, R. E. Mewis, D. C. Williamson, G. G. R. Green (**2012**) *Prog. Nucl. Magn. Reson. Spectrosc.* 67:1-48
7. L. Sellies, R. L. E. G. Aspers, M. C. Feiters, F. P. J. T. Rutjes M. Tessari (**2021**) *Angew. Chem. Int. Ed. Engl.* 60:26954-26959
8. A. Dey *et al.* (**2020**) *Anal. Chem.* 92:14867-14871
9. S. Jannin, J.-N. Dumez, P. Giraudeau, D. Kurzbach (**2019**) *J. Magn. Reson.* 305:41-50
10. R. Fraser, F. P. J. T. Rutjes, M. C. Feiters, M. Tessari (**2022**) *Acc. Chem. Res.* 55:1832-1844
11. L. T. Kuhn, J. Bargon (**2007**) *Top. Curr. Chem.* 276:125-154
12. L. T. Kuhn (**2013**) *Top. Curr. Chem.* 338:229-300
13. J. H. Lee, Y. Okuno, S. Cavagnero (**2014**) *J. Magn. Reson.* 241:18-31
14. Y. Okuno, M. F. Mecha, H. Yang, L. Zhu, C. G. Fry, S. Cavagnero (**2019**) *Proc. Natl. Acad. Sci. USA* 116:11602-11611
15. H. Yang, S. Li, C. A. Mickles, V. Guzman-Luna, K. Sugisaki, C. M. Thompson, H. H. Dang, S. Cavagnero (**2022**) *J. Am. Chem. Soc.* DOI: 10.1021/jacs.2c01809
16. M. Goez, K. H. Mok, P. J. Hore (**2005**) *J. Magn. Reson.* 177:236-246
17. P. J. Hore, R. W. Broadhurst (**1993**) *Prog. Nucl. Magn. Reson. Spectrosc.* 25:345-402
18. S. Bouatra, F. Aziat, R. Mandal, *et al.* (**2013**) *PLoS ONE* 9:e73076
19. Y. Okuno, S. Cavagnero (**2017**) *eMagRes* 6: 283-313
20. D. S. Wishart *et al.* (**2021**) *Nucl. Acids Res.* 50:D622-D631
21. S. Aygen *et al.* (**2014**) *JIMD Rep.* 16:101-111
22. S. Stob, R. Kaptein (**1989**) *Photochem. Photobiol.* 49:565-577
23. E. L. Ulrich; H. Akutsu; J. F. Doreleijers; Y. Harano; Y. E. Ioannidis; J. Lin; M. Livny; S. Mading; D. Maziuk; Z. Miller; E. Nakatani; C. F. Schulte; D. E. Tolmie; R. Kent Wenger; H. Yao; J. L. Markley (**2008**) *Nucl. Acids Res.* 36:D402-D408
24. N. Psychogios *et al.* (**2011**) *PLoS ONE* 6:e16957
25. Even though the optimisation of the photo-CIDNP-derived signal enhancement was lying beyond the scope of the proof-of-concept study presented here, signal enhancement factors obtained for hyperpolarised ^{1}H metabolite nuclei were determined wherever possible (Supporting Information; Table S2). We anticipate that significantly higher enhancements will be obtained via introducing specific measures aimed at maximising the signal-to-noise ratio of a photo-CIDNP experiment.
26. The ^{1}H CPMG experiment is routinely carried out during NMR metabolomic analyses of human serum to eliminate resonances from molecular species that contain rapidly relaxing nuclear spins, e.g. proteins and lipids.
27. B. Widner, M. Ledochowski, D. Fuchs (**2000**) *Lancet* 355:755-756

28. A. McCann, D. Aarsland, P. Magne Ueland, S.-E. H. Solvang, J. E. Nordrehaug, L. M. Giil (**2021**) *Brain Res.* 1765:147481
29. S. Engelborghs, B. Marescau, P. P. De Deyn (**2003**) *Neurochem. Res.* 28:1145-1150
30. A. Curti *et al.* (**2007**) *Blood* 109:2871-2877
31. F. Torres, A. Renn, R. Riek (**2021**) *Magn. Reson.* 2:321-329
32. J. E. Bramham, A. P. Golovanov (**2022**) *Commun. Chem.* 5:90